A Computationally Efficient, Volterra Series Based, ROM Method for Aeroelastic Systems With Stronger Aerodynamic Nonlinearities

Maciej Balajewicz, Fred Nitzsche and Daniel Feszty
Carleton University
Ottawa, CANADA

mbalajew@connect.carleton.ca

ABSTRACT

The following paper presents an alternate, more computationally viable Volterra series based, reduced-order-modeling approach for aerodynamic systems with stronger nonlinearities. The method is applied to a two-dimensional transonic airfoil undergoing high-amplitude, forced pitch harmonic oscillations. Unlike the standard Volterra series approach, the proposed method does not require the successive identification of computationally costly, higher-order Volterra kernels. Instead, stronger nonlinearities are captured through the identification of multiple, low-order Volterra kernels.

1.0 Introduction

Transonic aeroelasticity relies heavily on Computational Fluid Dynamics (CFD) for solutions to the complex, and inherently nonlinear transonic flow field. Unfortunately, the large computational resources associated with CFD solutions significantly inhibit the approach. As a result, interest in reduced-order-models (ROMs) of the transonic aerodynamic system has been significant [1–3]. Although research into the Volterra series as a ROM for the transonic aerodynamic system has been considerable [1, 4–11], in his recent review paper, Silva suggests that several critical issues remain unresolved.

1. **Volterra series for MDOF aerodynamic systems –** Silva states that "An important issue that needs to be addressed is the simultaneous excitation of multiple degrees of freedom in order to properly identify any nonlinear cross-coupling of the degrees of freedom" [2]. All previous applications of the Volterra series to multi-degree-of-freedom aerodynamic systems has been limited to the identification of aerodynamic nonlinearities resulting from individual perturbations of structural modes. Determination of total lift and moment for simultaneous motions required the superposition of the individual nonlinear responses. However, as suggested by Silva, the nonlinear nature of the system renders the principle of superposition invalid.

2. **Volterra series convergence –** Silva states that "...potential disadvantages of the Volterra theory include input amplitude limitations related to convergence issues and the need for higher-order

kernels" [2]. Identification of Volterra kernels is a resource intensive endeavor; limiting most aerodynamic applications to second-order truncations of the Volterra series. Unfortunately, such low-ordered series are applicable to weakly nonlinear systems only. For transonic aerodynamic applications, this requirement translates to small structural perturbations in low Mach number transonic flow regimes.

A method which addresses the problem of Volterra series modeling of MDOF aerodynamic systems has recently been proposed [12]. The purpose of the present paper is to introduce and summarize a method which addresses the problem of Volterra series convergence. The proposed method features a novel approach to the modeling of single-input nonlinear systems using the dual-input Volterra series. Instead of necessitating the identification of higher-order kernels, the proposed method relies on the identification of multiple, low-ordered Volterra kernels. Although a rigorous proof of this approach is not provided in this paper, encouraging preliminary results are presented. First, a simple nonlinear, first-order differential equation is modeled for illustrative purposes. Then, the applicability of the proposed method to nonlinear aerodynamic systems is illustrated by modeling the transonic, unsteady, two-degree-of-freedom airfoil undergoing high amplitude, forced pitch harmonic oscillations.

The organization of this paper is as follows. First, in section 2.0, the standard, single-input Volterra series approach to single-input systems is presented. This section describes the disadvantages of the single-input Volterra series and summarizes the motivation behind the method proposed in this paper. This new method, from here on refereed to as the dual-input Volterra series ROM method, is introduced in section 3.0. Finally, sections 4.0 and 5.0 contain results of the single and dual-input Volterra series ROMs of the example problem and the unsteady transonic airfoil respectively.

2.0 Volterra Theory

The Volterra theory of nonlinear systems is quite mature and several texts are available [13, 14]. It was first applied to nonlinear engineering problems by Wiener [15] and first applied to the transonic aerodynamic system by Silva [8].

The output $y(t)$ of a continuous-time, causal, time-invariant, fading memory, nonlinear system Ψ, due to a single-input $x(t)$

$$y(t) = \Psi\{x(t)\} \tag{1}$$

can be modeled using the p^{th}-order, Volterra series

$$\begin{aligned} y(t) &= \sum_{i=1}^{p} \mathbb{H}_i \\ &= \int_{-\infty}^{t} H_1(t-\tau)x(\tau)d\tau \\ &+ \int_{-\infty}^{t}\int_{-\infty}^{t} H_2(t-\tau_1, t-\tau_2)x(\tau_1)x(\tau_2)d\tau_1 d\tau_2 \\ &\vdots \\ &+ \int_{-\infty}^{t}\cdots\int_{-\infty}^{t} H_p(t-\tau_1,\cdots,t-\tau_p)\prod_{i=1}^{p}\{x(\tau_i)d\tau_i\} \end{aligned} \tag{2}$$

where the p^{th}-order Volterra operator $\mathbb{H}_p$, is defined as a p-fold convolution between the input $x(t)$ and the p^{th}-order Volterra kernel $H_p(t, \cdots, t)$. Due to the inherent and exponentially increasing difficulty of identifying higher-order kernels, especially when computational simulations are used, most aerodynamic applications use a truncated, second-order ($p = 2$) Volterra series

$$\begin{aligned} y(t) &= \int_{-\infty}^{t} H_1(t-\tau)x(\tau)d\tau \\ &+ \int_{-\infty}^{t}\int_{-\infty}^{t} H_2(t-\tau_1, t-\tau_2)x(\tau_1)x(\tau_2)d\tau_1 d\tau_2 \end{aligned} \tag{3}$$

The identification of Volterra kernels is key to the synthesis of a Volterra ROM. However, analytical derivations of the Volterra kernels in continuous-time are only possible if analytical, closed-form expression of the input-output relationship of the nonlinear system Ψ are available. Unfortunately, many engineering applications of interest including aerodynamic applications, lack such closed-form formulations and instead, rely on numerical solutions of the nonlinear system Ψ. As a result, identification of the Volterra kernels involves the processing of discrete-time outputs due to specifically tailored training inputs. Consequently, the discrete-time version of the Volterra series utilizing discrete-time Volterra operators and kernels, is preferred. For a uniformly sampled, discrete-time representation of the system

$$y[n] = \Psi\{x[n]\} \tag{4}$$

where

$$x[n] = x(t)|_{t=n\Delta T} = x(n\Delta T) \tag{5}$$

$$y[n] = y(t)|_{t=n\Delta T} = y(n\Delta T) \tag{6}$$

and $n = 0, 1, \cdots, N$. Hence, a second-order ($p = 2$), discrete-time Volterra series is of the form

$$\begin{aligned} y[n] &= \sum_{k=0}^{n} H_1[n-k]x[k] \\ &+ \sum_{k_1=0}^{n}\sum_{k_2=0}^{n} H_2[n-k_1, n-k_2]x[k_1]x[k_2] \end{aligned} \tag{7}$$

The first and second-order Volterra kernels can be identified using the unit-pulse identification method

$$H_1[n] = 2\Psi\{\delta[n]\} + \frac{1}{2}\Psi\{2\delta[n]\} \tag{8}$$

$$\sum_{k=0}^{N} \left(\begin{array}{rcl} 2H_2[n, n-k] & = & \Psi\{\delta[n] + \delta[n-k]\} \\ & - & \Psi\{\delta[n]\} - \Psi\{\delta[n-k]\} \end{array} \right) \tag{9}$$

where $\delta[n]$ is the unit-pulse function; discrete-time version of the impulse function

$$\delta[n] = \begin{cases} 1 & n = 0 \\ 0 & n \neq 0 \end{cases} \tag{10}$$

The identification of the first-order kernel $H_1[n]$ is straightforward. Only two outputs due to inputs $\delta[n]$ and $2\delta[n]$ are required. The identification of the second-order kernel $H_2[n, n]$, is more involved since multiple outputs due to inputs $\delta[n]$ and $\delta[n-k]$ for $k = 0, 1, \cdots, N$ must be computed. Due to symmetry, for all k

$$H_2[n, n-k] = H_2[n-k, n] \tag{11}$$

A second-order Volterra series ROM is adequate for weakly nonlinear systems. However, modeling stronger nonlinearities requires the identification and inclusion of higher-order kernels. Due to the inherent difficulties associated with the identification of higher-order kernels, this is often not feasible. In this paper, an alternate method of increasing the accuracy of a second-order Volterra ROM is presented.

3.0 Dual-Input Volterra ROM of Single-Input Systems

The multi-input Volterra series has been traditionally applied to multi-degree-of-freedom systems [16–21], including aerodynamic multi-degree-of-freedom systems [12]. The method proposed in this paper utilizes the multi-input series for single-input systems by artificially subdividing a single-input system

$$y[n] = \Psi\{x[n]\} \tag{12}$$

into a dual-input system

$$y[n] = \Psi\{x_1[n], x_2[n]\} \tag{13}$$

where the two inputs $x_1[n]$ and $x_2[n]$ are the positive and negative components of $x[n]$

$$\begin{array}{ll} x_1[n] = x[n] & \text{if } x[n] \geq 0 \\ x_1[n] = 0 & \text{if } x[n] < 0 \end{array} \tag{14}$$

$$\begin{array}{ll} x_2[n] = 0 & \text{if } x[n] \geq 0 \\ x_2[n] = x[n] & \text{if } x[n] < 0 \end{array} \tag{15}$$

We assume the output $y[n]$, of the single-input system can modeled using a second-order, dual-input Volterra series of the artificial dual-input system

$$\begin{aligned}
y[n] &= \sum_{j=1}^{2}\left\{\sum_{k=0}^{n} H_1^j[n-\tau]x_j[k]\right\} \\
&+ \sum_{j_1=1}^{2}\sum_{j_2=1}^{2}\left\{\sum_{k_1=0}^{n}\sum_{k_1=0}^{n} H_2^{j_1 j_2}[n-k_1, n-k_2]x_{j_1}[k_1]x_{j_2}[k_2]\right\} \\
&= \sum_{k=0}^{n} H_1^1[n-\tau]x_1[k] + \sum_{k=0}^{n} H_1^2[n-\tau]x_2[k] \\
&+ \sum_{k_1=0}^{n}\sum_{k_1=0}^{n} H_2^{11}[n-k_1, n-k_2]x_1[k_1]x_1[k_2] \\
&+ \sum_{k_1=0}^{n}\sum_{k_1=0}^{n} H_2^{22}[n-k_1, n-k_2]x_2[k_1]x_2[k_2] \\
&+ \sum_{k_1=0}^{n}\sum_{k_1=0}^{n} H_2^{12}[n-k_1, n-k_2]x_1[k_1]x_2[k_2] \\
&+ \sum_{k_1=0}^{n}\sum_{k_1=0}^{n} H_2^{21}[n-k_1, n-k_2]x_2[k_1]x_1[k_2]
\end{aligned} \tag{16}$$

It should be noted that the superscripts appearing on the first and second-order, dual-input Volterra kernels identify to which inputs, $x_1(t)$ or $x_2(t)$, the kernel corresponds to. For example, the second-order Volterra kernel, H_2^{12}, corresponds to both the $x_1(t)$ and $x_2(t)$ inputs, while the second-order Volterra kernel, H_2^{22}, corresponds to the input $x_2(t)$ only. The first and second-order, dual-input Volterra kernels can be identified using Eq. 17 and 18

$$\sum_{j=1}^{2}\left(H_1^j[n] = 2\Psi\{\delta_j[n]\} + \frac{1}{2}\Psi\{2\delta_j[n]\}\right) \tag{17}$$

$$\sum_{j_1=1}^{2}\sum_{j_2=1}^{2}\left\{\sum_{k=0}^{N}\left(\begin{array}{rcl} 2H_2^{j_1 j_2}[n, n-k] &=& \Psi\{\delta_{j_1}[n] + \delta_{j_2}[n-k]\} \\ &-& \Psi\{\delta_{j_1}[n]\} - \Psi\{\delta_{j_2}[n-k]\} \end{array}\right)\right\} \tag{18}$$

The identification process for the dual-input kernels uses both positive and negative unit-pulse functions

$$\begin{aligned}
\delta_1[n] &= \begin{cases} 1 & n = 0 \\ 0 & n \neq 0 \end{cases} \\
\delta_2[n] &= \begin{cases} -1 & n = 0 \\ 0 & n \neq 0 \end{cases}
\end{aligned} \tag{19}$$

Due to symmetry, for all k.

$$\begin{aligned}
H_2^{j_1 j_2}[n, n-k] = H_2^{j_1 j_2}[n-k, n] \quad \text{for} \quad j_1 = j_2 \\
H_2^{j_1 j_2}[n, n-k] = H_2^{j_2 j_1}[n-k, n] \quad \text{for} \quad j_1 \neq j_2
\end{aligned} \tag{20}$$

The following section demonstrates the capabilities of the dual-input Volterra series ROM method using a simple example problem.

4.0 Example Problem

Consider a single-input $x(t)$, single-output $y(t)$ system Ψ

$$y(t) = \Psi\{x(t)\} \tag{21}$$

described by the following nonlinear differential equation

$$\dot{y}(t) + y(t) + ky(t)^2 = x(t) \tag{22}$$

where

$$k = \begin{cases} 0.5 & y(t) > 0 \\ 0 & y(t) \leq 0 \end{cases} \tag{23}$$

The "exact" output $y(t)$, of Eq. 22 is determined using a second-order backward in time, finite difference model with a time step Δt, equal to $2\pi/30$.

4.1 Second-Order, Single-Input Volterra ROM of Example Problem

The second-order, single-input Volterra series ROM of the example problem is of the form

$$\begin{aligned} y[n] &= \sum_{k=0}^{n} H_1[n-k]x[k] \\ &+ \sum_{k_1=0}^{n}\sum_{k_2=0}^{n} H_2[n-k_1, n-k_2]x[k_1]x[k_2] \end{aligned} \tag{24}$$

The first and second-order, single-input Volterra kernels H_1 and H_2, are identified using Eq. 8 and Eq. 9 respectively.

4.2 Second-Order, Dual-Input Volterra ROM of Example Problem

The second-order, dual-input Volterra series ROM of the example problem is of the form

$$\begin{aligned} y[n] &= \sum_{j=1}^{2}\left\{\sum_{k=0}^{n} H_1^j[n-\tau]x_j[k]\right\} \\ &+ \sum_{j_1=1}^{2}\sum_{j_2=1}^{2}\left\{\sum_{k_1=0}^{n}\sum_{k_1=0}^{n} H_2^{j_1 j_2}[n-k_1, n-k_2]x_{j_1}[k_1]x_{j_2}[k_2]\right\} \end{aligned} \tag{25}$$

where the single input is subdivided into its positive and negative components

$$\begin{array}{ll} x_1[n] = x[n] & \text{if } x[n] \geq 0 \\ x_1[n] = 0 & \text{if } x[n] < 0 \end{array} \tag{26}$$

$$\begin{array}{ll} x_2[n] = 0 & \text{if } x[n] \geq 0 \\ x_2[n] = x[n] & \text{if } x[n] < 0 \end{array} \quad (27)$$

The first and second-order, dual-input Volterra kernels H_1^1, H_1^2 and $H_2^{11}, H_2^{22}, H_2^{12}, H_2^{21}$ are identified using Eq. 17 and 18 respectively.

4.3 Example Problem Results

Figure 1 illustrates the steady-state output of the finite difference and Volterra ROM models of the example problem for a sinusoidal input

$$x[n] = \sin[n\Delta t] \quad (28)$$

The thick gray curve plots the "exact", finite-difference solution of the example problem. The thin black curve illustrates the output as predicted by a second-order, single-input Volterra series ROM. The dotted curve corresponds to the system response as predicted by a second-order, dual-input Volterra series ROM. It is clear that for this specific example, the second-order, dual-input Volterra ROM is significantly more accurate then the second-order, single-input Volterra ROM.

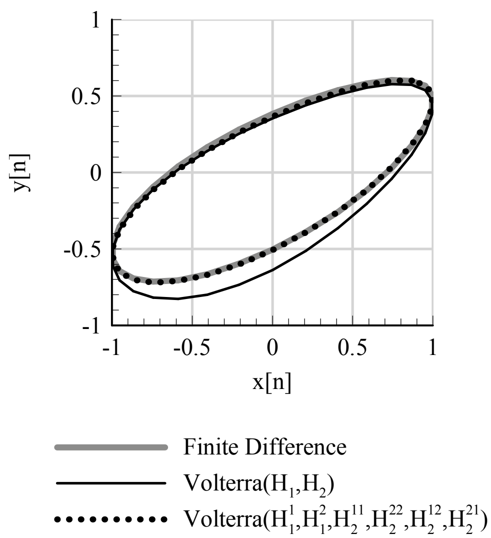

Figure 1: Example problem results

5.0 Unsteady Transonic Airfoil

Coefficients of lift $C_L[n]$, and moment $C_M[n]$, fully characterize the aerodynamics of a two-dimensional NACA0012 airfoil oscillating in pitch $\alpha[n]$. For the sake of brevity, in this paper we limit our discussion to the aerodynamic moment output only. The "exact" solution is determined using the Carleton Multi Block (CMB) CFD code

$$C_M[n] = \text{CFD}\{\alpha[n]\} \quad (29)$$

The CMB code is a derivative of a code originally developed at the University of Glasgow, specifically tailored for transonic, time marching aeroelastic analysis. For further details, refer to Dubuc et al [22] and Badcock et al [23]. The aerodynamics of the airfoil were modeled using the inviscid Euler equations. The two-dimensional airfoil domain was discretized using a C type 180x33 Euler grid with 130 nodes on the airfoil. The surface nodes were a distance of approximately $0.001c$ off the airfoil surface, where c is the airfoil chord. The mesh extended into the far field approximately $10c$ in all directions. The unsteady solutions were solved using 20 time steps per each period of the airfoil pitch oscillation. This choice of mesh and time step was based on several studies on mesh refinement carried out by Dubuc et al., which showed that no significant accuracy improvements are gained at higher spatial or temporal mesh densities [22].

5.1 Second-Order, Single-Input Volterra ROM of Unsteady Transonic Airfoil

A second-order, single-input Volterra series ROM of the unsteady aerodynamic system is of the form

$$\begin{aligned} C_M[n] &= \sum_{k=0}^{n} H_1[n-k]\alpha[k] \\ &+ \sum_{k_1=0}^{n}\sum_{k_2=0}^{n} H_2[n-k_1, n-k_2]\alpha[k_1]\alpha[k_2] \end{aligned} \tag{30}$$

The first and second-order, single-input Volterra kernels H_1 and H_2, are identified using Eq. 8 and Eq. 9; reproduced here for convenience

$$H_1[n] = 2\mathrm{CFD}\{\delta[n]\} + \frac{1}{2}\mathrm{CFD}\{2\delta[n]\} \tag{31}$$

$$\sum_{k=0}^{N}\left(\begin{array}{rcl} 2H_2[n, n-k] & = & \mathrm{CFD}\{\delta[n]+\delta[n-k]\} \\ & - & \mathrm{CFD}\{\delta[n]\} - \mathrm{CFD}\{\delta[n-k]\} \end{array}\right) \tag{32}$$

where $\delta[n]$ is the unit-pulse function in pitch

$$\delta[n] = \begin{cases} 1 & n = 0 \\ 0 & n \neq 0 \end{cases} \tag{33}$$

5.2 Second-Order, Dual-Input Volterra ROM of Unsteady Transonic Airfoil

A second-order, single-input Volterra series ROM of the unsteady aerodynamic system is of the form

$$\begin{aligned} C_M[n] &= \sum_{j=1}^{2}\left\{\sum_{k=0}^{n} H_1^{j}[n-\tau]\alpha_j[k]\right\} \\ &+ \sum_{j_1=1}^{2}\sum_{j_2=1}^{2}\left\{\sum_{k_1=0}^{n}\sum_{k_1=0}^{n} H_2^{j_1 j_2}[n-k_1, n-k_2]\alpha_{j_1}[k_1]\alpha_{j_2}[k_2]\right\} \end{aligned} \tag{34}$$

where the single-input, single-output system

$$C_M = \mathrm{CFD}\{\alpha[n]\} \tag{35}$$

is artificially subdivided into a dual-input system

$$C_M = \text{CFD}\{\alpha_1[n], \alpha_2[n]\} \tag{36}$$

where the two inputs $\alpha_1[n]$ and $\alpha_2[n]$, are the positive and negative components of $\alpha[n]$

$$\begin{array}{ll} \alpha_1[n] = \alpha[n] & \text{if } \alpha[n] \geq 0 \\ \alpha_1[n] = 0 & \text{if } \alpha[n] < 0 \end{array} \tag{37}$$

$$\begin{array}{ll} \alpha_2[n] = 0 & \text{if } \alpha[n] \geq 0 \\ \alpha_2[n] = \alpha[n] & \text{if } \alpha[n] < 0 \end{array} \tag{38}$$

The first and second-order, dual-input Volterra kernels $H_1^1, H_1^2, H_2^{11}, H_2^{22}, H_2^{12}$, and H_2^{21} are identified using Eq. 17 and 18; reproduced here for convenience

$$\sum_{j=1}^{2} \left(H_1^j[n] = 2\text{CFD}\{\delta_j[n]\} + \frac{1}{2}\text{CFD}\{2\delta_j[n]\} \right) \tag{39}$$

$$\sum_{j_1=1}^{2} \sum_{j_2=1}^{2} \left\{ \sum_{k=0}^{N} \left(\begin{array}{rcl} 2H_2^{j_1 j_2}[n, n-k] & = & \text{CFD}\{\delta_{j_1}[n] + \delta_{j_2}[n-k]\} \\ & - & \text{CFD}\{\delta_{j_1}[n]\} - \text{CFD}\{\delta_{j_2}[n-k]\} \end{array} \right) \right\} \tag{40}$$

The identification method uses both positive and negative unit-impulse functions in pitch

$$\begin{array}{l} \delta_1[n] = \begin{cases} 1 & n = 0 \\ 0 & n \neq 0 \end{cases} \\ \delta_2[n] = \begin{cases} -1 & n = 0 \\ 0 & n \neq 0 \end{cases} \end{array} \tag{41}$$

5.3 Unsteady Transonic Airfoil Results

We choose to model the AGARD-R-702 [24], CT2 test case which features the NACA0012 airfoil oscillating in pitch about its quarter-chord

$$\alpha(t) = 3.16^\circ + 4.59^\circ \sin(\omega_\alpha t) \tag{42}$$

at a Mach number $M = 0.6$ and a reduced frequency $k_\alpha = 0.081$, defined as

$$k = \frac{\omega_\alpha c}{2U_\infty} \tag{43}$$

where U_∞ is the constant forward velocity of the airfoil in terms of the Mach number M. Figure 2 compares the experimental and CFD outputs of the AGARD test case; very good agreement was obtained. Errors are likely associated with the neglect of viscous forces and uncertainties in the experimental data [22]. Figure 3 illustrates the instantaneous pressure coefficient C_P distributions along the upper and lower surfaces of the NACA0012 airfoil. This particular pitch motion results in the formation of a strong shockwave experiencing Tijdeman's [25] Type B shock motion. Figure 4 shows the steady-state CFD and Volterra ROM moment coefficient outputs. The thick gray curve illustrates the "exact" CFD solution. The thin black curve illustrates the output as predicted by the second-order,

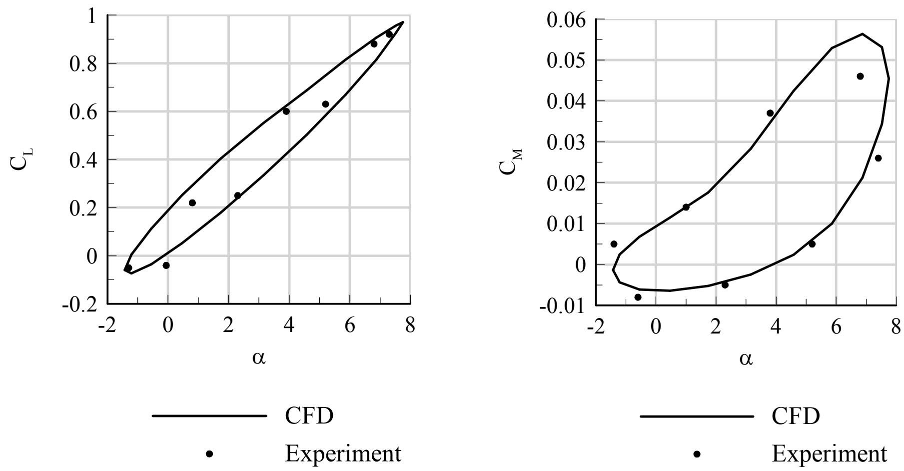

(a) Lift coefficient (b) Moment coefficient

Figure 2: CFD validation using AGARD CT2 test case experimental results

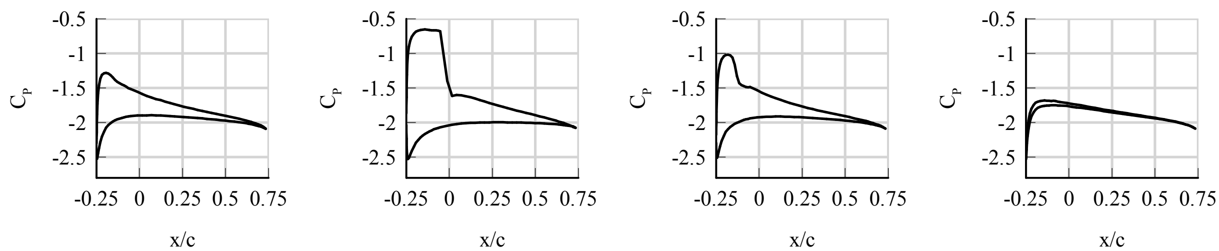

(a) $\alpha = 3.16°$, up (b) $\alpha = 7.75°$ (c) $\alpha = 3.16°$, down (d) $\alpha = -1.43°$

Figure 3: Instantaneous pressure coefficient C_P distributions for the AGARD CT2 test case

single-input Volterra series ROM. The dotted curve corresponds to the system response as predicted by the second-order, dual-input Volterra series ROM. For this specific test case, the second-order, dual-input Volterra series ROM of Eq. 34, shows significant accuracy improvements over the second-order, single-input Volterra series ROM. We can quantify the modeling performance of the Volterra ROMs using the L^2 relative error norm, given as

$$\text{Error} = \sqrt{\frac{\{\text{CFD} - \text{Volterra ROM}\}^2}{\{\text{CFD}\}^2}} \times 100 \tag{44}$$

Error norms for the Volterra ROMs covered in this paper are summarized in Table 1.

6.0 Conclusion

The following paper presented an alternate, more computationally viable Volterra series based, reduced-order-modeling approach for aerodynamic systems with stronger nonlinearities. The method is applied to a two-dimensional transonic airfoil undergoing high-amplitude, forced pitch harmonic os-

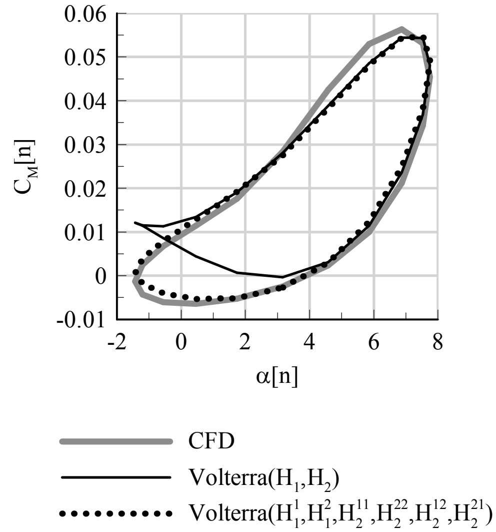

Figure 4: Volterra ROMs of AGARD CT2 test case

Table 1: Volterra ROM modeling error norms

ROM	Error [%]
Volterra(H_1, H_2)	24.7
Volterra($H_1^1, H_1^2, H_2^{11}, H_2^{22}, H_2^{12}, H_2^{21}$)	8.7

cillations. It has been demonstrated that this approach can considerably increase the accuracy of a standard second-order Volterra ROM with out the identification of the costly third-order kernel.

REFERENCES

[1] Lucia, D., Beran, P., and Silva, W., "Reduced-Order Modeling: New Approached for Computational Physics," *Progress in Aerospace Sciences*, Vol. 40, 2003, pp. 51–117.

[2] Silva, W., "Identification of Nonlinear Aeroelastic Systems Based on the Volterra Theory: Progress and Opportunity," *Nonlinear Dynamics*, Vol. 39, No. 1–2, 2005.

[3] Dowell, E., Edwards, J., and Strganac, T., "Nonlinear Aeroelasticity," *Journal of Aircraft*, Vol. 40, No. 5, 2003.

[4] Beran, P. S. and Silva, W. A., "Reduced-order Modeling: New Approaches for Computational Physics," *39th AIAA Aerospace Sciences Meeting*, Reno, Nevada, Jan. 2001.

[5] Lucia, D. J., Beran, P. S., and Silva, W. A., "Aeroelastic System Development Using Proper Orthogonal Decomposition and Volterra Theory," *44th Structures, Structural Dynamics and Materials Conference*, Norfolk, Virginia, 2003.

[6] Raveh, D. E., Levy, Y., and Karpel, M., "Aircraft Aeroelastic Analysis and Design Using CFD-based Unsteady Loads," *41st Structures, Structural Dynamics, and Materials Conference*, Atlanta, Georgia, 2000.

[7] Raveh, D. E., "Reduced Order Models for Nonlinear Unsteady Aerodynamics," AIAA paper 2000–4785, 2000.

[8] Silva, W., "Application of Nonlinear Systems Theory to Transonic Unsteady Aerodynamic Responses," *Journal of Aircraft*, Vol. 30, No. 5, 1993.

[9] Silva, W., "Reduced-order Models Based on Linear and Nonlinear Aerodynamic Impulse Responses," *CEAS/AIAA/ICASE/NASA International Forum on Aeroelasticity and Structural Dynamics*, 1999.

[10] Silva, W., Beran, P. S., Cesnik, C. E. S., Kurdila, R. E., Prazenica, A., Librescu, R. J., Marzocca, P., and Raveh, D., "Reduced-order Modeling: Cooperative Research and Development at the NASA Langley Research Center," *CEAS/AIAA/ICASE/NASA International Forum on Aeroelasticity and Structural Dynamics*, Reno, Nevada, 2001.

[11] Silva, W., Hong, M. S., Bartels, R. E., Piatak, D. J., and Scott, R. C., "Identifcation of Computational and Experimental Reduced-order Models," *International Forum on Aeroelasticity and Structural Dynamics*, Amsterdam, 2003.

[12] Balajewicz, M., Nitzsche, F., and Feszty, D., "On the Application of Multi-Input Volterra Theory to Nonlinear Multi-Degree-of-Freedom Aerodynamic Systems," *49th AIAA/ASME/ASCE/AHS/ASC Structures, Structural Dynamics, and Materials Conference*, No. AIAA-2008-2324, Schaumburg, IL, April 2008.

[13] Rugh, W. J., *Nonlinear System Theory. The Volterra/Wiener Approach*, The John Hopkins University Press, 1981.

[14] Schetzen, M., *The Volterra and Wiener Theories of Nonlinear Systems*, New York: Wiley, 1980.

[15] Wiener, N., "Response of a Nonlinear Device to Noise," Report no. 129, Radiation Laboratory, M.I.T., Cambridge, Mass., 1942.

[16] Grzymacz, N. M. and Koch, C., "Functional Properties of Models for Direction Selectivity in the Retina," *Synapse*, Vol. 1, No. 5, 1987, pp. 417–434.

[17] Agarossi, L., Agarossi, L., Bellini, S., Canella, A., and Migliorati, P., "A Volterra Model for the High Density Optical Disc," *Proc. IEEE International Conference on Acoustics, Speech and Signal Processing*, edited by S. Bellini, Vol. 3, 1998, pp. 1605–1608 vol.3.

[18] Dimoka, A., Courellis, S. H., Marmarelis, V. Z., and Berger, T. W., "Modeling the Interactions of Two Major Extrinsic Pathways and Their Output to the Granule Cells of the Hippocampus of the Mammalian Brain," *SBE's International Conference on Bimolecular Engineering*, 2007.

[19] Chatterjee, A. and Vyas, N. S., "Nonlinear Parameter Estimation in Multi-Degree-of-Freedom Systems Using Multi-Input Volterra Series," *Mechanical Systems and Signal Processing*, Vol. 18, 2004, pp. 457–489.

[20] Marmarelis, P. Z. and Naka, K. I., "Identification of Multi-Input Biological Systems," *Biomedical Engineering, IEEE Transactions on*, Vol. BME-21, March 1974, pp. 88–101.

[21] Worden, K., Manson, G., and Tomlinson, G. R., "A Harmonic Probing Algorithm for the Multi-Input Volterra Series," *Journal of Sound and Vibration*, Vol. 201, No. 1, 1997, pp. 67–84.

[22] Dubuc, L., Cantariti, F., Woodgate, M., Gribben, B., Badcock, K. J., and Richards, B. E., "Solution of the Euler Unsteady Equations Using Deforming Grids," Aero. report 9704, University of Glasgow, 1997.

[23] Badcock, K. J., Richards, B. E., and Woodgate, M. A., "Elements of Computational Fluid Dynamics on Block Structured Grids Using Implicit Solvers," *Progress in Aerospace Sciences*, Vol. 36, No. 5, 2000, pp. 351–392.

[24] "Compendium of Unsteady Aerodynamic Measurements," Tech. rep., AGARD-R-702, 1982.

[25] Tijdeman, H. and Seebass, R., "Transonic Flow Past Oscillating Airfoils," *Ann. Rev. Fluid Mech.*, Vol. 12, 1980, pp. 181–222.